MOLECULAR AND CELLULAR BIOLOGY, Oct. 1998, p. 6063–6074 Vol. 18, No. 10
0270-7306/98/$04.00+0

FGF-18, a Novel Member of the Fibroblast Growth Factor Family, Stimulates Hepatic and Intestinal Proliferation

MICKEY C.-T. HU,[1]* WAN R. QIU,[1] YOU-PING WANG,[1] DAVE HILL,[2] BRIAN D. RING,[2] SHEILA SCULLY,[2] BRAD BOLON,[2] MARGARET DEROSE,[3] ROLAND LUETHY,[4] W. SCOTT SIMONET,[3] TSUTOMU ARAKAWA,[5] AND DIMITRY M. DANILENKO[2]

Departments of Cell Biology,[1] Pathology,[2] Molecular Genetics,[3] Computational Biology,[4] and Protein Chemistry,[5] Amgen, Inc., Thousand Oaks, California 91320

Received 13 March 1998/Returned for modification 27 April 1998/Accepted 1 July 1998

The fibroblast growth factors (FGFs) play key roles in controlling tissue growth, morphogenesis, and repair in animals. We have cloned a novel member of the FGF family, designated FGF-18, that is expressed primarily in the lungs and kidneys and at lower levels in the heart, testes, spleen, skeletal muscle, and brain. Sequence comparison indicates that FGF-18 is highly conserved between humans and mice and is most homologous to FGF-8 among the FGF family members. FGF-18 has a typical signal sequence and was glycosylated and secreted when it was transfected into 293-EBNA cells. Recombinant murine FGF-18 protein (rMuFGF-18) stimulated proliferation in the fibroblast cell line NIH 3T3 in vitro in a heparan sulfate-dependent manner. To examine its biological activity in vivo, rMuFGF-18 was injected into normal mice and ectopically overexpressed in transgenic mice by using a liver-specific promoter. Injection of rMuFGF-18 induced proliferation in a wide variety of tissues, including tissues of both epithelial and mesenchymal origin. The two tissues which appeared to be the primary targets of FGF-18 were the liver and small intestine, both of which exhibited histologic evidence of proliferation and showed significant gains in organ weight following 7 (sometimes 3) days of FGF-18 treatment. Transgenic mice that overexpressed FGF-18 in the liver also exhibited an increase in liver weight and hepatocellular proliferation. These results suggest that FGF-18 is a pleiotropic growth factor that stimulates proliferation in a number of tissues, most notably the liver and small intestine.

The fibroblast growth factors (FGFs) form a family of heparin-binding growth factors and oncogenes with at least 18 structurally related members (reviewed in references 6, 11, and 30). Individual FGFs play important roles in various physiological and pathological processes, including embryonic development, cell growth, morphogenesis, tissue repair, inflammation, angiogenesis, and tumor growth and invasion (30). The first characterized members of the FGF family were acidic FGF (aFGF or FGF-1) and basic FGF (bFGF or FGF-2), which were purified as mitogens for fibroblasts from the pituitary and brain (7, 9, 12, 23, 41). Subsequently, it became apparent that these growth factors were able to promote the growth of mesodermal and neuroectodermal cells during both embryogenesis and adulthood (14, 15). Indeed, morphogenic events involving the epithelium and the underlying mesenchyme have now become a hallmark of the functions of each FGF family member. While FGFs may affect the pattern of differentiation of ectodermal precursor cells in early embryos (24, 40), the function of FGFs is often to stimulate tissue repair (wound healing) in the adult (5, 8). This repair function may be mobilized in the presence of certain pathological conditions, for instance, diseases of the retina, muscular dystrophy, rheumatoid arthritis, and Alzheimer's disease (reviewed in reference 13). Furthermore, it appears that inappropriate or altered expression of FGFs and their receptors occurs in the presence of a variety of cancers, including many common carcinomas (1, 2, 10, 18, 19, 27, 28, 32, 33, 43, 50).

FGF family members use a dual receptor system to exert their cellular effects. The signal-transducing subunit is a family of FGF receptors (FGFRs). The other subunit is heparan sulfate (HS) proteoglycan at the cell surface (25, 37). HS, the most structurally complex glycosaminoglycan made by animal cells, is chemically related to heparin but markedly different from it in uronic acid content and extent of sulfation (21). Heparin can activate the mitogenic activity of several FGFs (26, 37) but inhibits that of some FGFs (16, 35). Moreover, the effect of heparin on FGF mitogenic activity appears to be cell type-dependent and remains to be elucidated (16, 38). Since heparin is a pharmaceutical product derived from proteoglycans within intracellular vesicles (21), it is probably not a physiological activator of FGFs. The full definition of the structures involved in the interactions between FGFs and their cognate receptors, as well as the consequences of these interactions, will lead to a greater understanding, at the molecular level, of the role that FGFs play in developmental and pathological processes.

Here we report the isolation, characterization, and functional study of a novel mouse and human member of the FGF family, designated FGF-18. Structural analysis revealed that FGF-18 is highly conserved between humans and mice and is most similar to FGF-8 (42) among the FGF family members. The purified recombinant murine FGF-18 (rMuFGF-18) protein was biologically active in vitro and in vivo. Similar to FGF-2 (17, 22, 34, 48), rMuFGF-18 stimulated proliferation in a fibroblast cell line, NIH 3T3, in a cell-associated HS-dependent manner. In particular, functional studies of rMuFGF-18 protein in vivo showed that FGF-18 is a pleiotropic growth factor that stimulated proliferation in many cell types and a wide variety of tissues, including tissues of both epithelial and mesenchymal origin. However, the two tissues which appeared to be the primary targets of rMuFGF-18 were those of the liver and the small intestine.

* Corresponding author. Mailing address: Amgen, Inc., 14-1-D, Thousand Oaks, CA 91320. Phone: (805) 447-6721. Fax: (805) 447-1982. E-mail: mhu@amgen.com.

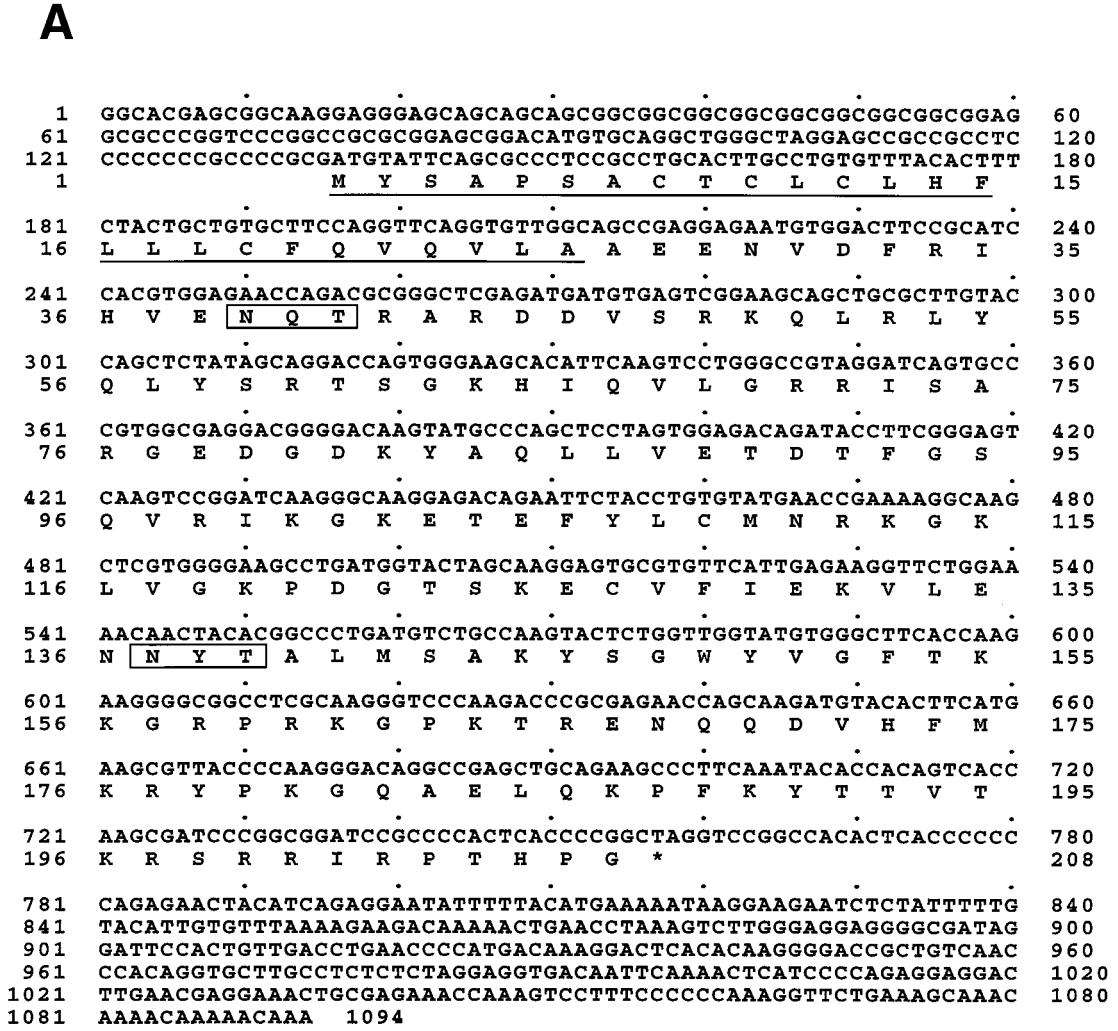

FIG. 1. Sequence analysis. (A) The deduced amino acid sequence of mouse FGF-18 is indicated below the first nucleotide of each codon, and the termination codon is marked with an asterisk. The predicted signal peptide is underlined, and the potential N-glycosylation sites are boxed. (B) The predicted amino acid sequence of the mouse FGF-18 (mFGF-18) was compared with those of human FGF-18 (hFGF-18), FGF-17, and FGF-8 (performed with the PileUp program of the Genetics Computer Group sequence analysis software package). Amino acids that are identical in all of the sequences are shown in black boxes. (C) Phylogenetic analysis of the FGF family tree, linking members with closely homologous amino acid sequences. Phenogram representation of the inferred phylogenetic tree based on degree of amino acid sequence homology is shown. Branch lengths are arbitrary. GenBank accession numbers: human FGF-1, P05230; human FGF-2, P09038; human FGF-3, P11487; human FGF-4, P08620; human FGF-5, P12034; human FGF-6, P10767; human FGF-7, P21781; human FGF-8, P55075; human FGF-9, P31371; human FGF-10, AB002097; human FGF-11, Q92914; human FGF-12, Q92912; human FGF-13, Q92913; human FGF-14, Q92915; mouse FGF-15, AF007268; human FGF-16, AB009391; human FGF-17, AB009249; human FGF-18, AF075292.

MATERIALS AND METHODS

Isolation of full-length mouse and human FGF-18 cDNAs and sequence analysis. A novel mouse expressed sequence tag (EST) cDNA fragment of 495 bp with significant homology to human FGF-8 and FGF-9 was identified in the Amgen EST database. This EST cDNA was used as a probe to screen a mouse kidney cDNA library in the λUni-ZAP XR phage vector (Stratagene, Inc., La Jolla, Calif.). For hybridization, replicate filters were prehybridized for 1 h at 68°C in Express hybridization buffer (Clontech Laboratories, Inc., Palo Alto, Calif.) and hybridized overnight in the same solution with the [^{32}P]dCTP-labeled probe. After hybridization, the filters were washed several times at high stringency, at 65°C in 0.2× SSPE (1× SSPE is 0.18 M NaCl, 10 mM NaH_2PO_4, and 1 mM EDTA [pH 7.7])–0.1% sodium dodecyl sulfate (SDS), and subjected to autoradiography. Twenty positive clones were picked and purified after screening 4×10^6 phages. The cDNA inserts of these positive phage clones were subsequently converted into pBluescript SK− plasmid vector by using the in vivo excision method with the ExAssist helper phage as specified by the manufacturer (Stratagene, Inc.). After analysis of the inserts, four long (full-length) clones were sequenced on both strands by a PCR procedure involving fluorescent dideoxynucleotides and a model 373A automated sequencer (Applied Biosystems, Foster City, Calif.). For human FGF-18 cDNA cloning, the full-length mouse FGF-18 cDNA was used as a probe to screen a human heart λTripEx cDNA library (Clontech Laboratories, Inc.). Several positive clones were obtained, and the cDNA inserts of these phage clones were subsequently converted in vivo into pTripEx plasmid vector, as specified by the manufacturer (Clontech Laboratories, Inc.). The full-length cDNA clones were sequenced on both strands as described above. Sequence comparisons were performed with the Bestfit program or aligned with the PileUp program of the Genetics Computer Group sequence analysis software package (Wisconsin Package version 9.0).

Western blot and Northern blot analyses. The culture media from 293-EBNA cells or the pCEP/FGF-18/Flag-expressing cells were collected and analyzed by Western blot analysis. After SDS-polyacrylamide gel electrophoresis (10% polyacrylamide) (PAGE), protein samples were electroblotted onto a polyvinylidene difluoride membrane (Novex, Inc., San Diego, Calif.) and probed with the anti-Flag M2 monoclonal antibody (MAb) (Kodak Scientific Imaging Systems, New Haven, Conn.). Immunocomplexes were visualized by enhanced chemiluminescence detection (Amersham, Inc., Arlington Heights, Ill.) with goat anti-mouse antiserum conjugated with horseradish peroxidase as a secondary antibody (Pierce, Rockford, Ill.). Mouse and human multiple-tissue Northern blots containing poly(A)$^+$ RNA (2 μg/lane) from a variety of different tissues were purchased from Clontech Laboratories, Inc. Mouse or human FGF-18 cDNA

B

```
mFGF-18   MYSAPSACTCLCLHFLLLCFQVQVLAAEE.....................  29
hFGF-18   MYSAPSACTCLCLHFLLLCFQVQVLVAEE.....................  29
hFGF-17   MGAARLLPNLTLCLQLLILCCQTQGENHP.....................  29
hFGF-8    MGSPRSALSCLLLHLLVLCLQAQVRSAAQKRGPGAGNPADTLGQGHEDRP  50

mFGF-18   ..............................NVDFRIHVENQTRARDDVS  48
hFGF-18   ..............................NVDFRIHVENQTRARDDVS  48
hFGF-17   ..............................SPNFNQYVRDQGAMTDQLS  48
hFGF-8    FGQRSRAGKNFTNPAPNYPEEGSKEQRDSVLPKVTQRHVREQSLVTDQLS  100

mFGF-18   RKQLRLYQLYSRTSGKHIQVL.GRRISARGEDGDKYAQLLVETDTFGSQV  97
hFGF-18   RKQLRLYQLYSRTSGKHIQVL.GRRISARGEDGDKYAQLLVETDTFGSQV  97
hFGF-17   RRQIREYQLYSRTSGKHVQVT.GRRISATAEDGNKFAKLIVETDTFGSRV  97
hFGF-8    RRLIRTYQLYSRTSGKHVQVLANKRINAMAEDGDPFAKLIVETDTFGSRV  150

mFGF-18   RIKGKETEFYLCMNRKGKLVGKPDGTSKECVFIEKVLENNYTALMSAKYS  147
hFGF-18   RIKGKETEFYLCMNRKGKLVGKPDGTSKECVFIEKVLENNYTALMSAKYS  147
hFGF-17   RIKGAESEKYICMNKRGKLIGKPSGKSKDCVFTEIVLENNYTAFQNARHE  147
hFGF-8    RVRGAETGLYICMNKKGKLIAKSNGKGKDCVFTEIVLENNYTALQNAKYE  200

mFGF-18   GWYVGFTKKGRPRKGPKTRENQQDVHFMKRYPKGQAELQKPFKYTTVTKR  197
hFGF-18   GWYVGFTKKGRPRKGPKTRENQQDVHFMKRYPKGQPELQKPFKYTTVTKR  197
hFGF-17   GWFMAFTRQGRPRQASRSRQNQREAHFIKRLYQGQLPFPNHAEKQKQFEF  197
hFGF-8    GWYMAFTRKGRPRKGSKTRQHQREVHFMKRLPRGHHTTEQSLRFEFLNYP  250

mFGF-18   SRRIRPTHPG          207
hFGF-18   SRRIRPTHPA          207
hFGF-17   VGSAPTRRTKRTRRPQPLT 216
hFGF-8    PFTRSLRGSQRTWAPEPR  268
```

C

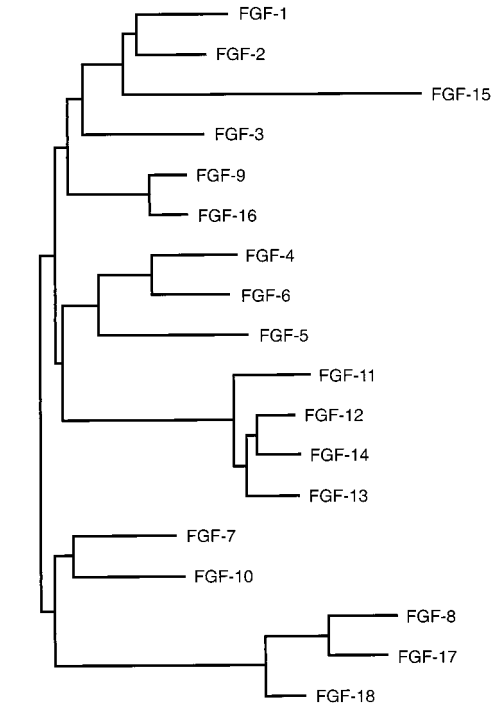

was labeled with [^{32}P]dCTP to a specific activity of approximately 10^8 dpm/μg. Membranes were hybridized with either the mouse or human FGF-18 cDNA probe, washed at high stringency (65°C in 0.2× SSPE–0.1% SDS), and subjected to autoradiography.

In situ hybridization. Radiolabeled antisense or sense transcript was synthesized from the linearized mouse FGF-18 cDNA plasmid with T7 or T3 RNA polymerase (Promega, Inc., Madison, Wis.), respectively, and [^{33}P]rUTP (Amersham, Inc.). In situ hybridization was performed as previously described (49). Slides were counterstained with hematoxylin and eosin (H&E) and photographed under dark-field illumination.

Purification of rMuFGF-18 protein. Mouse FGF-18 cDNA (amino acids 27 to 207) was subcloned into the bacterial expression vector by PCR with the forward and reverse primers 5′-TATTCTAGAGCCGAGGAGAATGTGGACTTCCG C-3′ and 5′-TATCTCGAGCTAGCCGGGGTGAGTGGGGCGGATC-3′, and the resulting plasmid was designated pAMG/FGF-18. This plasmid was introduced into *Escherichia coli* GM221 (Amgen, Inc., Thousand Oaks, Calif.). The *E. coli* cells were mechanically lysed in water with a Gaulin homogenizer, and the lysate was centrifuged at 10,000 rpm for 2 h. The supernatant was mixed with an S-Sepharose resin (Pharmacia, Inc., Piscataway, N.J.) equilibrated in 50 mM Tris (pH 8.0). After a 30-min incubation at 4°C with slow stirring, the resin was transferred into a sintered glass filter. It was then extensively washed with the same buffer and packed into a column. After a further wash in the column with the same buffer followed by a wash with 0.5 M NaCl–50 mM Tris (pH 8.0), the bound proteins were eluted with a linear NaCl gradient from 0.5 to 3 M in the same Tris buffer. The fractions containing rMuFGF-18, as determined by SDS-PAGE, were eluted at 2 M NaCl. These fractions were pooled and dialyzed against 10 mM sodium phosphate (pH 7.0) with a Spectra/Por 3,000-molecular-weight-cutoff dialysis membrane. After several changes of dialysis buffer, the protein solution was loaded onto a freshly packed S-Sepharose column (equilibrated with 10 mM sodium phosphate [pH 7.0]). The bound proteins were eluted with a linear NaCl gradient from 0.5 to 3 M in the same (phosphate) buffer. The fractions containing greater than 90% rMuFGF-18 were pooled and dialyzed against the phosphate-buffered saline with the same dialysis membrane, filtered under sterile conditions, and stored at 4°C.

Production and deglycosylation of mammalian rMuFGF-18. Full-length mouse FGF-18 cDNA (amino acids 1 to 207) was cloned into the mammalian expression vector pCEP4 (Invitrogen, Inc., Carlsbad, Calif.) by PCR with the two forward and reverse primers 5′-TATAAGCTTGGTACCGCCACCATGTATT CAGCGCCCTCCGCC-3′ and 5′-TATTGCGGCCGCTTATCATTTATCATC ATCATCTTTATAATCGCCGGGGTGAGTGGGGCGGATC-3′. The second primer included a Flag tag at the 3′ end, and the resulting plasmid was designated pCEP/FGF-18/Flag. 293-EBNA cells were grown in Dulbecco's modified Eagle's medium (DMEM) (GibcoBRL, Gaithersburg, Md.) supplemented with 10% fetal bovine serum (FBS) (GibcoBRL). Cells to be transfected were plated at a density of 2×10^6 cells per 100-mm dish the day before transfection. 293-EBNA cells were transfected with expression plasmid (10 μg per dish) by using the calcium phosphate precipitation protocol (Specialty Media, Inc.). The

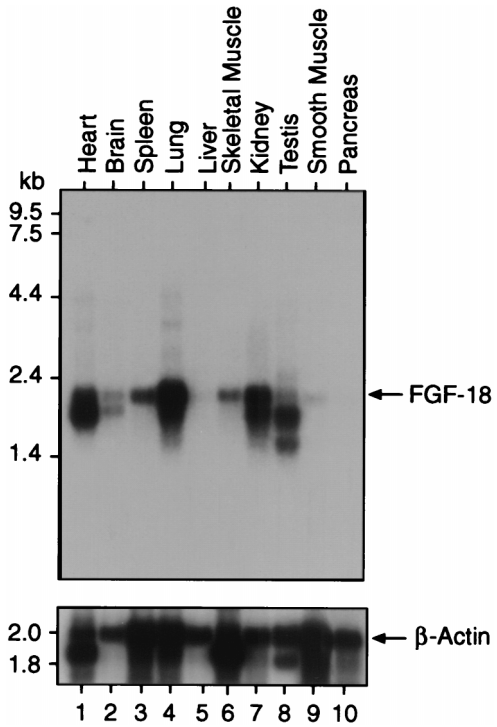

FIG. 2. Expression patterns of mouse FGF-18. Northern blots of various mouse tissues were probed with the mouse FGF-18 cDNA. As a control, the same blots were reprobed with β-actin cDNA to check the integrity of the RNA (bottom panel). The specific transcripts are highlighted.

positive cell clones were isolated by hygromycin B (Boehringer Mannheim Biochemicals, Indianapolis, Ind.) selection and expanded.

For deglycosylation experiments, FGF-18F-producing 293-EBNA cells were treated with tunicamycin (Sigma Chemical Co., St. Louis, Mo.) or the conditioned media containing mammalian FGF-18F protein were treated with various deglycosylation enzymes including neuraminidase, *N*-glycanase, and *O*-glycanase (Oxford GlycoSciences, Inc., Wakefield, Mass.). The treated mammalian FGF-18F protein was examined by Western blot analysis with anti-Flag M2 MAb.

Heparin-binding assay. Cell lysate containing rMuFGF-18 protein was passed through a heparin-Sepharose (Pharmacia, Inc.) column. After extensive washing, the bound proteins were eluted with 2 M NaCl, electrophoresed, transferred to a polyvinylidene difluoride membrane, and probed with anti-rMuFGF-18 antibody. A separate heparin-binding experiment was performed with a Biospecific Interaction Analysis (BIAcore) instrument (Pharmacia Biosensor, Piscataway, N.J.). FGF-2 or rMuFGF-18 protein was immobilized on a CM5 sensor chip on a BIAcore instrument, and binding assays were performed in 10 mM HEPES (pH 7.5)–150 mM NaCl–2.4 mM EDTA with heparin (20 μg/ml); the runs were 30 to 35 μl of analyte at a flow rate of 5 μl/min, as specified by the manufacturer.

NIH 3T3 cell proliferation assay in vitro. NIH 3T3 cells were cultured in DMEM supplemented with 10% FBS in the absence or presence of 30 mM sodium chlorate (Sigma Chemical Co.) (34). The cells were collected by trypsinization, and a cell suspension (7,500 cells per 100 μl) was dispensed into each well of 96-well tissue culture microtiter plates (Falcon, Becton Dickinson Labware, Lincoln Park, N.J.). After 24 h, the medium was changed to DMEM–0.1% FBS (starvation medium), and culturing was continued for 24 h. Growth factors (rMuFGF-18 or FGF-2) were added to each well at this time, and 5-bromo-2′-deoxyuridine (BrdU) (Boehringer Mannheim) was added to each well after 16 h. (Recombinant human FGF-2 was included in these assays as a positive control, while phosphate-buffered saline was used as a negative control.) After a 5-h incubation, the cells were fixed for 30 min at −20°C with 70% ethanol containing 0.5 M HCl. Subsequently, DNA synthesis was assayed quantitatively by measuring BrdU incorporation into cellular DNA with an anti-BrdU antibody by using a standard cell enzyme-linked immunosorbent assay (ELISA) protocol. The cells were treated with nuclease solution for 30 min at 37°C, washed, and incubated for 30 min at 37°C with the anti-BrdU antibody labeled with peroxidase (Boehringer Mannheim). After being washed, the samples were incubated with peroxidase substrate at room temperature for 15 min. The absorbance at 490 nm of the samples was determined by using a scanning multiwell spectrophotometer (ELISA reader; Molecular Devices, Corp., Sunnyvale, Calif.) with the excitation at 405 nm. Similarly, the tetrazolium MTS cell proliferation assay (Promega, Inc.) was performed as specified by the manufacturer.

Necropsy, clinical pathology, and histopathology. Eighteen 8-week-old female BDF1 mice were divided into six groups of three mice each (one treated and one control group injected once daily for either 1, 3, or 7 days). Treatments consisted of intraperitoneal injections with either 5 mg of rMuFGF-18 or vehicle per kg. At 1 h before necropsy, all the mice were injected intraperitoneally with 50 mg of BrdU per kg. At necropsy, the mice were radiographed, blood was collected, body and selected organ weights were measured, and tissues were harvested for routine histological and cell proliferation (BrdU-labeling) analyses. Serum was analyzed for clinical chemistries on a Hitachi 717 system (Boehringer Mannheim), and complete blood cell counts were obtained from whole blood with a Technicon H1E analyzer (Miles Technicon Instrument Corp., Tarrytown, N.Y.). Zinc formalin (Anatech, Battle Creek, Mich.)-fixed tissues were embedded in paraffin, sectioned at 4 μm, and stained with H&E. Data from the rMuFGF-18-injected mice at each of the three time points were analyzed with respect to data pooled from all nine control mice by using an unpaired Student *t* test (see Table 1).

Immunohistochemistry and cell proliferation analysis in tissues. Nuclear BrdU incorporation was assessed on serial 4-mm-thick paraffin sections. An automated staining method was used with a TechMate Immunostainer (BioTek Solutions, Santa Barbara, Calif.). Tissue sections were digested with 0.1% protease (Sigma Chemical Co.) followed by 2 N HCl. BrdU was detected with a rat MAb to BrdU followed by a biotinylated anti-rabbit/anti-mouse secondary cocktail (BioTek) and an avidin and biotinylated horseradish peroxidase macromolecular complex (ABC) tertiary coupled to alkaline phosphatase (BioTek). The staining reaction was visualized with BioTek Red chromagen (BioTek). BrdU-labeled hepatocytes were quantified manually by investigators blinded to the treatment group, by counting BrdU-labeled hepatocytes in 10 noncontiguous, randomly chosen microscopic high-power fields (HPF) (40× objective) per liver section to determine the mean number of BrdU-positive hepatocytes per HPF.

Preparation and analysis of transgenic mice. The coding region for the mouse FGF-18 cDNA was subcloned into an expression vector, placing it under control of the human ApoE promoter and liver-specific enhancer (39). For microinjection, the ApoE–FGF-18 plasmid was purified through two rounds of equilibrium centrifugation in CsCl. The plasmid was digested with *Cla*I and *Ase*I, and the 3.3-kb transgene insert was purified on a 0.8% ultrapure DNA agarose gel (FMC) by electrophoresis onto NA 45 paper. The purified fragment was diluted to 1 to 2 μg/ml in 5 mM Tris (pH 7.4)–0.2 mM EDTA. Single-cell embryos from $BDF_1 \times BDF_1$-bred mice were injected essentially as described previously (4). Embryos were cultured overnight in a CO_2 incubator, and 15 to 20 two-cell embryos were transferred to the oviducts of pseudopregnant CD1 female mice. Of 77 offspring generated from implantation of microinjected embryos, 11 were identified as transgenic founders by screening for the ApoE–FGF-18 transgene in DNA prepared from ear or tail biopsy specimens. The 11 founders were necropsied (as described above) at 6 to 8 weeks of age. Northern analysis of total RNA from snap-frozen liver revealed six expressors (two males and four females). Transgene mRNA levels were measured by semiquantitative Northern analysis and classified as "high," "medium," or "low" based on relative band signal intensity (*n* represents the number of animals). Two female and three male mice lacking the transgene were used as control animals. Blood and tissues were evaluated as described above, with the exception of cell proliferation. In this experiment, semiautomated counts of total hepatocyte nuclei were obtained in five random fields by using a 20× objective and Metamorph image analysis software (Universal Imaging, West Chester, Pa.). Data were analyzed with JMP statistical software (version 3.2.1; SAS Institute, Cary, N.C.). Values were examined by genotype in nonparametric tests.

Nucleotide sequence accession number. The FGF-18 sequence has been submitted to GenBank and given accession no. AF075291.

RESULTS

Molecular cloning and structure of mouse and human FGF-18 cDNA. A 495-bp partial mouse cDNA sequence with significant homology to FGF-8 was identified from an Amgen EST database derived from a mouse fetal lung cDNA library. Using this mouse cDNA as a probe, we have isolated two full-length cDNA clones from a mouse kidney cDNA library. The nucleotide sequence of 1,094 bp contains a single open reading frame of 621 bp encoding a polypeptide of 207 amino acids, with a calculated molecular mass of ~23 kDa (Fig. 1A). After the ATG initiation codon, there is a stretch of 27 hydrophobic amino acids with the characteristics of a signal peptide (47) and two potential N-linked glycosylation sites with the consensus sequence N-X-S/T, suggesting that it is a candidate secreted glycoprotein. A homology search of the available databases did not reveal any amino acid sequence identical to that of this clone. However, the deduced amino acid sequence of this cDNA is substantially homologous to those of FGF

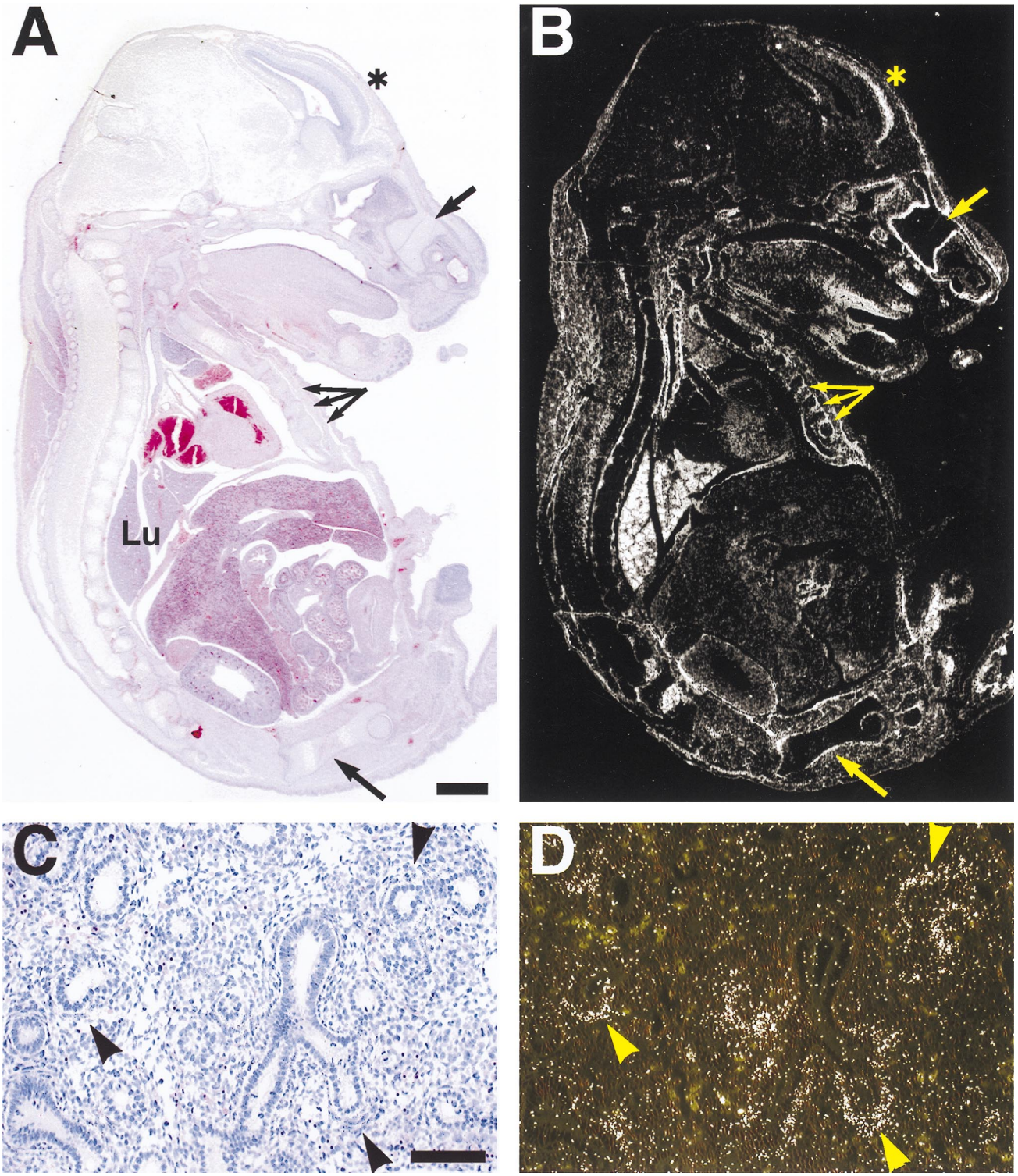

FIG. 3. In situ hybridization analysis of FGF-18 mRNA expression in E15.5 mouse embryo. (A) Sagittal section counterstained with H&E. Lu, lung. (B) In situ hybridization of the same sagittal section. The strongest signal was found in the lung. Arrows indicate signals surrounding developing bones, and the asterisk denotes signal in the cerebral cortex of the developing brain. Bar, 1 mm. (C) Higher magnification of the embryonic lung counterstained with H&E. (D) Higher magnification of in situ hybridization of the same area of panel C. Arrowheads indicate FGF-18 mRNA expression in areas of lung mesenchymal cells adjacent to airways. Bar, 100 μm.

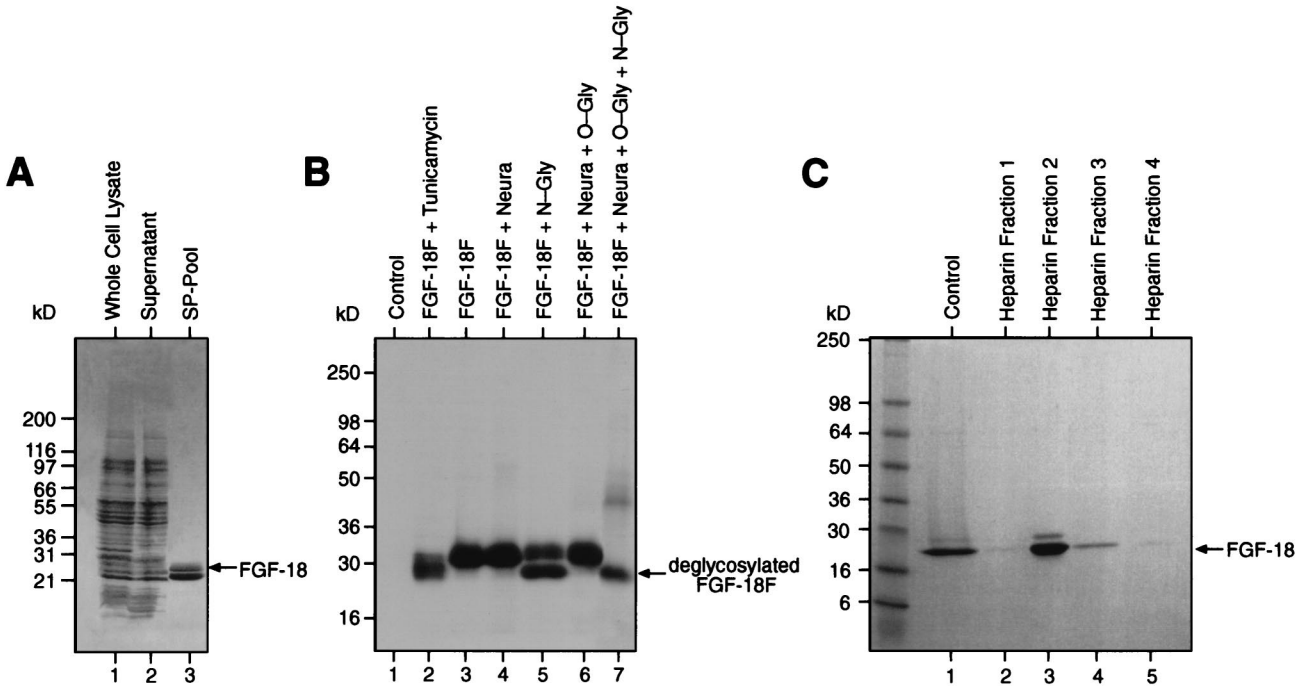

FIG. 4. rMuFGF-18 protein expressed in *E. coli* and human 293-EBNA cells. (A) Purification of the *E. coli*-derived rMuFGF-18 protein. The *E. coli* whole-cell lysate, the supernatant of the lysate, and the pooled sample from the second SP-Sepharose column were analyzed by SDS-PAGE and stained with Coomassie blue. (B) Western blot analysis and deglycosylation of the Flag-tagged FGF-18 (FGF-18F) protein produced in 293-EBNA cells. The serum-free conditioned media were collected from the FGF-18F-transfected 293-EBNA cells cultured in the absence or presence of 0.2 μg of tunicamycin per ml (lane 2). The conditioned media without preincubation with tunicamycin were treated with the indicated deglycosylation enzymes including neuraminidase (Neura), *N*-glycanase (N-Gly), and *O*-glycanase (O-Gly) (lanes 4 to 7) and examined by Western blot analysis with anti-Flag M2 MAb. (C) Detection of rMuFGF-18 binding to heparin by affinity chromatography. Cell lysate containing rMuFGF-18 was passed through a heparin-Sepharose column, and the bound proteins were eluted and immunoblotted with anti-rMuFGF-18 antibody. As a positive control for rMuFGF-18, an aliquot of rMuFGF-18 purified from *E. coli* was included (lane 1).

proteins, suggesting that it is a novel member of the FGF family. Therefore, we have designated this growth factor FGF-18.

Using the full-length mouse cDNA as a probe, we have also isolated two full-length cDNA clones from a human heart cDNA library. The deduced amino acid sequence of human FGF-18 is 99% identical to that of mouse FGF-18. In addition, human FGF-18 is 72% homologous (60% identical) to human FGF-8 and 69% homologous (58% identical) to FGF-17 (Fig. 1B); to a lesser extent, it is homologous to other FGF family members. The amino acid sequence alignments among the 18 known FGF family members were used to infer a phylogenetic tree (Fig. 1C) with the CLUSTAL W program (44), and FGF-18, FGF-17, and FGF-8 were grouped. Two cysteine residues (Cys109 and Cys127) in the secreted FGF-18, FGF-17, and FGF-8 proteins are conserved (Fig. 1B), and the Cys127 of FGF-18 is conserved throughout the entire FGF family (data not shown).

Expression of FGF-18 in various mouse tissues. To examine the tissue distribution of FGF-18, we investigated the level of FGF-18 mRNA in several adult mouse tissues by Northern blot analysis. Two distinct FGF-18 transcripts (approximately 2.2 and 1.8 kb) were identified primarily in the lungs and kidneys (Fig. 2). Lower-level expression of these two transcripts was detected in the heart, testis, spleen, skeletal muscle, and brain. These two transcripts were barely detected in smooth muscle and not readily detectable in the liver and pancreas. Furthermore, we examined the expression of FGF-18 mRNA in the mouse 15.5-day embryo by in situ hybridization with a ^{33}P-labeled antisense FGF-18 RNA probe followed by autoradiography. The strongest signal for FGF-18 was found in the lungs, primarily in areas of pulmonary mesenchymal cells adjacent to airways (Fig. 3). FGF-18 signal was also observed surrounding developing bones and in the cerebral cortex of the developing brain (Fig. 3A and B). The negative control hybridization with a ^{33}P-labeled sense FGF-18 RNA probe did not show any detectable signal (data not shown).

Analysis of rMuFGF-18 proteins produced in *E. coli* and mammalian cells. The rMuFGF-18 protein purified from *E. coli* showed two major bands on SDS-PAGE (Fig. 4A), with molecular masses of approximately 26 and 22 kDa. The amino acid sequence analysis of these two bands indicated that both forms of rMuFGF-18 contained the same N-terminal sequence, i.e., EENVDFRIHV, indicating that the smaller form is truncated at the C terminus. The 26-kDa form corresponds to the intact full-length protein, whereas the 22-kDa form lacks approximately 12 amino acids at the C terminus. Two independent preparations of rMuFGF-18 in *E. coli* showed that the 22-kDa protein was the major form, suggesting that it might be produced by proteolytic cleavage of the full-length protein at the C terminus.

To determine whether rMuFGF-18 could be secreted in mammalian cells, localization of the Flag-tagged FGF-18 (FGF-18F) protein in cultured 293-EBNA cells transfected with the FGF-18F expression vector was examined by Western blotting with anti-Flag M2 MAb. The reactive protein was detected primarily in the culture medium (Fig. 4B, lane 3). Moreover, the amino acid sequence analysis of the purified FGF-18F protein indicated that FGF-18F contained the N-terminal sequence of EENVDFRIHV as predicted. These data indicated that this protein was secreted from the cells with

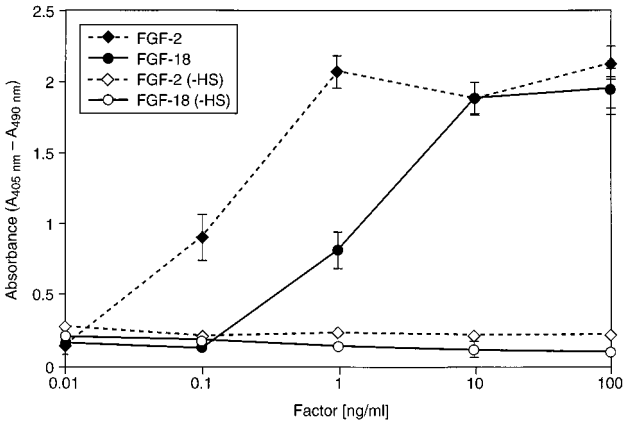

FIG. 5. Proliferation of NIH 3T3 cells in response to rMuFGF-18 and human FGF-2 by the BrdU-labeling procedures. Treatment of cells with sodium chlorate inhibited the sulfation of cell-associated HS proteoglycans (−HS). Increasing concentrations of rMuFGF-18 or FGF-2 were added into cell cultures with (open symbols) or without (solid symbols) preincubation with sodium chlorate. Proliferation was quantified by measuring the absorbance at 490 nm with a scanning multiwell spectrophotometer (ELISA reader). Error bars indicate the mean and standard deviation for triplicate assay values.

proper cleavage of the N-terminal signal peptide. To test whether glycosylation causes the difference in the molecular size between this mammalian protein (~32 kDa) and the full-length protein purified from *E. coli* (~26 kDa), FGF-18F-producing 293-EBNA cells were treated with tunicamycin and the secreted FGF-18F protein was examined by Western blotting with anti-Flag M2 MAb. As shown in Fig. 4B, the molecular mass of deglycosylated FGF-18F protein was about 28 kDa (lane 2). Since the FGF-18F protein contains an extra 1 kDa of the Flag peptide, the estimated molecular size of the deglycosylated mammalian FGF-18 is approximately the same as that of FGF-18 protein purified from *E. coli*. To confirm these results, the conditioned medium containing mammalian FGF-18F protein was treated with various deglycosylation enzymes as indicated (lanes 4 to 7). As expected, the N-linked oligosaccharides on mammalian FGF-18F protein could be removed by *N*-glycanase (lanes 5 and 7) but not by neuraminidase or *O*-glycanase (lanes 4 and 6) and the deglycosylated FGF-18F comigrated with the tunicamycin-treated FGF-18F (lane 2).

To examine whether rMuFGF-18 can bind to heparin, cell lysate containing rMuFGF-18 was passed through a heparin-Sepharose column and probed with anti-rMuFGF-18 antibody. The 22-kDa rMuFGF-18 proteins were detected in the bound fractions (Fig. 4C, lanes 3 and 4), indicating that rMuFGF-18 can bind to heparin specifically. Furthermore, BIAcore assays indicated that rMuFGF-18 bound to heparin or soluble HS more strongly than did FGF-2 (data not shown).

rMuFGF-18 stimulates proliferation of fibroblast cell lines in vitro. Since it has been well documented that FGF-1 and FGF-2 can strongly activate DNA synthesis in the NIH 3T3 fibroblast cell line (12, 36), we investigated whether rMuFGF-18 protein purified from *E. coli* could stimulate DNA synthesis in NIH 3T3 cells in culture. As shown in Fig. 5, rMuFGF-18 exerted a dose-dependent increase in DNA synthesis in NIH 3T3 cells, suggesting that it stimulates the proliferation of fibroblasts. In comparison to the negative control, half-maximal stimulation occurred at ~2 ng/ml and maximal stimulation occurred at ~10 ng/ml. Furthermore, similar results were obtained in the MTS cell proliferation assay (Promega, Inc.), where rMuFGF-18 showed a dose-dependent augmentation of NIH 3T3 cell growth (data not shown). The mitogenic activity of *E. coli*-derived rMuFGF-18 protein on NIH 3T3 cells was virtually the same as that of mammalian FGF-18F protein (data not shown). However, the specific activity of rMuFGF-18 on NIH 3T3 cells was considerably lower than that induced by FGF-2.

To determine whether cell-associated HS is required for the mitogenic activity of rMuFGF-18, NIH 3T3 cells were cultured in the same DMEM containing 30 mM sodium chlorate for 72 h to block sulfation of cell surface HS proteoglycans (34) and the same cell proliferation assays were performed. Strikingly, the mitogenic activity of rMuFGF-18 on NIH 3T3 cells was completely abolished after sodium chlorate treatment, suggesting that cell-associated HS is essential for rMuFGF-18 activity.

rMuFGF-18 increases the weights of the liver and small intestine and induces proliferation in many cell types in vivo. We next sought to determine whether FGF-18 modulated cell proliferation in vivo by injecting purified rMuFGF-18 protein into normal mice. As listed in Table 1, mice injected with rMuFGF-18 had significantly increased duodenal, jejunal, ileal, and hepatic wet weights after 7 days. There were also significant increases in the cholesterol levels in serum on days 1 and 7 and in the total protein and albumin levels in serum on day 7. There was a significant decrease in the alkaline phosphatase level in serum on both days 3 and 7. Histologically, rMuFGF-18 induced marked intestinal villus hypertrophy, characterized by an increase in both villus length and width, after 7 days of treatment (Fig. 6). In addition, an increase in BrdU nuclear labeling of

TABLE 1. Selected organ weights, serum chemistry, and hepatocellular BrdU labeling in mice injected with rMuFGF-18 at 5 mg/kg/day

Characteristic	Value in mice injected with[a]:			
	Vehicle (n = 9)	1 day of FGF-18 (n = 3)	3 days of FGF-18 (n = 3)	7 days of FGF-18 (n = 3)
Liver wt as % of body wt	4.87 ± 0.35	5.16 ± 0.49	4.97 ± 0.21	5.40 ± 0.42 (P = 0.05)
Duodenal wt as % of body wt	1.22 ± 0.04	1.31 ± 0.1	1.43 ± 0.16 (P = 0.01)	1.55 ± 0.1 (P = 0.0003)
Jejunal wt as % of body wt	2.10 ± 0.04	2.0 ± 0.14	2.41 ± 0.14	3.09 ± 0.41 (P = 0.0008)
Ileal wt as % of body wt	0.67 ± 0.04	0.68 ± 0.07	0.73 ± 0.06	0.89 ± 0.23 (P = 0.04)
Cholesterol concn (mg/dl)	64.6 ± 7.4	91 ± 12.5 (P = 0.001)	74 ± 6.1	77 ± 3.0 (P = 0.02)
Total protein concn in serum (mg/dl)	4.7 ± 0.1	4.9 ± 0.2	5.1 ± 0.3 (P = 0.009)	5.5 ± 0.2 (P < 0.0001)
Albumin concn in serum (mg/dl)	3.6 ± 0.2	3.7 ± 0.2	3.9 ± 0.2	4.1 ± 0.2 (P = 0.003)
Alkaline phosphatase activity (IU/liter)	135 ± 8	105 ± 18	80 ± 7 (P = 0.02)	70 ± 7 (P = 0.007)
No. of BrdU-positive hepatocytes per HPF	0.1 ± 0.3	6.3 ± 7.9 (P < 0.0001)	9.9 ± 3.8 (P < 0.0001)	2.5 ± 2.2 (P < 0.0001)

[a] Values represent mean ± standard deviation. P values indicate significance and are expressed relative to the values obtained with vehicle.

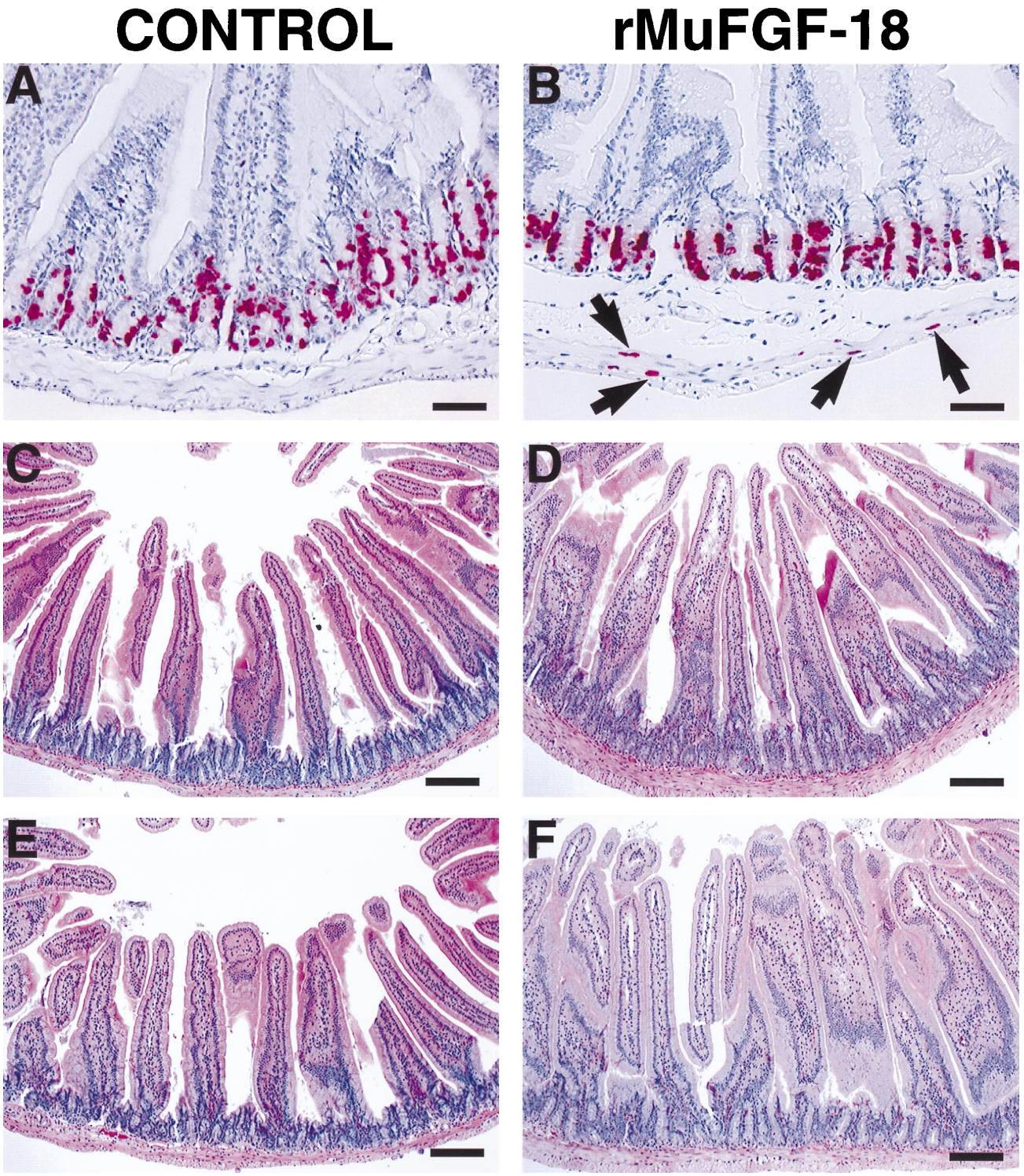

FIG. 6. Histologic analysis of rMuFGF-18-induced proliferation and mucosal hypertrophy in the small intestine. BrdU (A and B)- and H&E (C through F)-labeled sections of jejunum from mice injected with 5 mg of rMuFGF-18 per kg per day for 3 days (B) or 7 days (D and F) and mice injected with buffer control (A, C, and E) are shown. Panel B illustrates an increase in BrdU labeling of smooth muscle cells in the tunica muscularis of the rMuFGF-18-injected mouse (B) with respect to the buffer control-injected mouse (A), while panels D and F illustrate mucosal hypertrophy, characterized by an increase in jejunal villus length and thickness in the two mice injected with rMuFGF-18 for 7 days (D and F) with respect to the two buffer control-injected mice (C and E). Bars, 50 μm (A and B) and 100 μm (C through F).

hepatocytes, urinary bladder transitional urothelium, and pancreatic ductal and acinar epithelial cells was observed (Table 1; Fig. 7). rMuFGF-18 increased the number of BrdU-labeled smooth muscle cells in the tunica muscularis of the intestine (Fig. 6B) and urinary bladder (Fig. 7D) and the number of BrdU-labeled fibroblasts and smooth muscle cells in the pancreatic interstitium (Fig. 7F). These results indicate that rMuFGF-18 induces proliferation in a wide

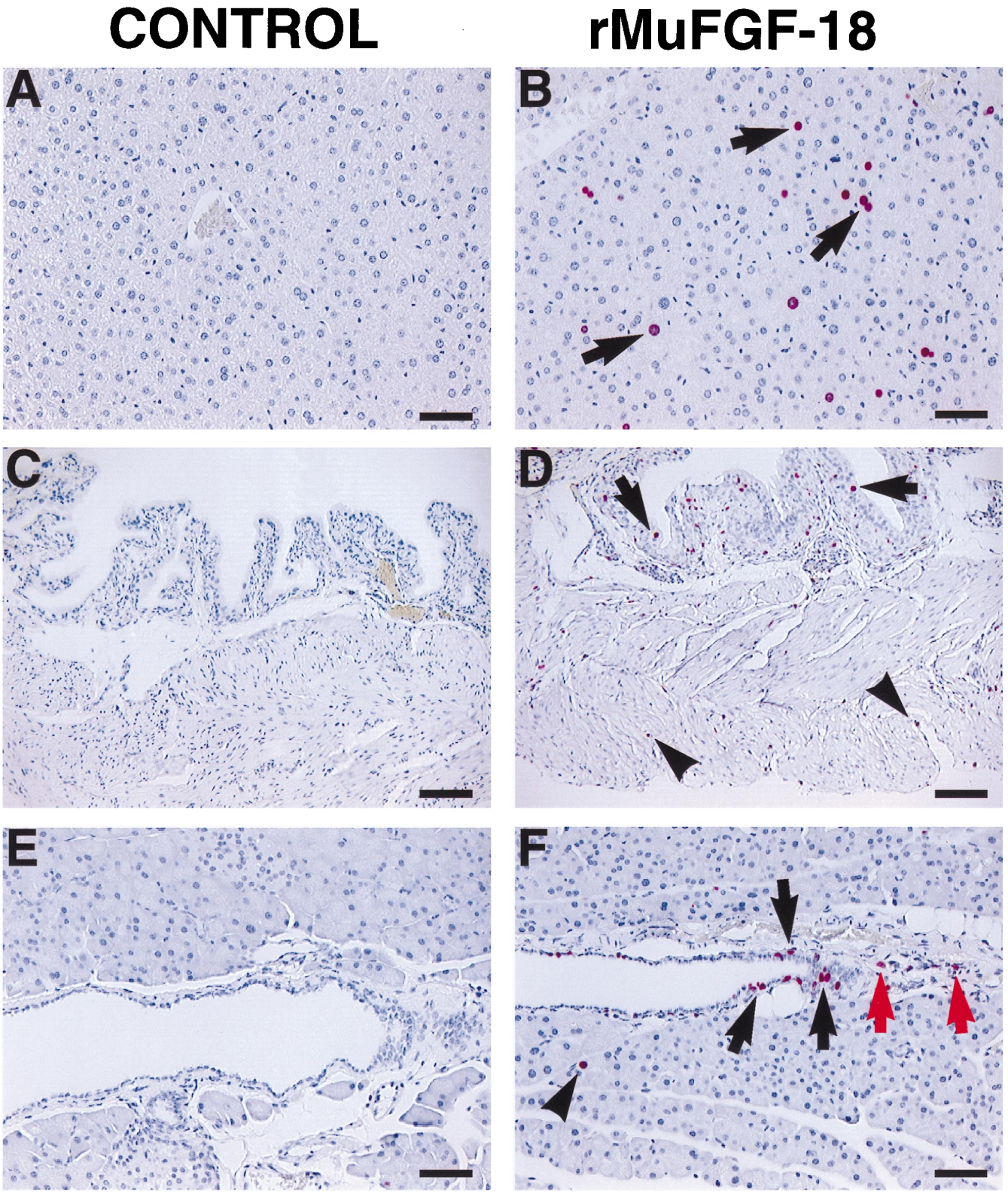

FIG. 7. Histologic analysis of rMuFGF-18-induced proliferation in the liver. Immunohistochemical results of BrdU labeling in sections of liver (A and B), urinary bladder (C and D), and pancreas (E and F) from mice injected with 5 mg of rMuFGF-18 per kg per day for 3 days (B, D, and F) and mice injected with buffer control for 3 days (A, C, and E) are shown. Panel B illustrates an increase in hepatocellular BrdU labeling (arrows) in the rMuFGF-18-injected mouse (B) with respect to the buffer control-injected mouse (A). Panel D illustrates an increase in BrdU labeling of the transitional urothelium (arrows) and smooth muscle cells in the tunica muscularis (arrowheads) of the rMuFGF-18-injected mouse (D) with respect to the buffer control-injected mouse (C). Panel F illustrates an increase in BrdU labeling of pancreatic ductal epithelium (black arrows), pancreatic acinar epithelium (black arrowhead), and fibroblasts and smooth muscle cells in the pancreatic interstitium (red arrowheads), of the rMuFGF-18-injected (F) mouse with respect to the buffer control-injected mouse (E). Bars, 50 μm (A, B, E, and F) and 100 μm (C and D).

TABLE 2. Liver weights and number of hepatocyte nuclei per HPF in transgenic mice with hepatic overexpression of FGF-18

Hepatic FGF-18 expression level	No. of mice tested	Liver wt (% of body wt)[a]	No. of hepatocyte nuclei/HPF[a]
High	2	6.28 ± 0.40	140 ± 4[b]
Moderate	3	5.67 ± 0.66	114 ± 8[b]
Low	1	5.55	111
None	5	5.60 ± 0.56	91 ± 7

[a] Values represent mean ± standard deviation.
[b] Significantly different from nonexpressing mice ($P < 0.05$).

variety of tissues, including tissues of both epithelial and mesenchymal origin.

In a separate study, MuFGF-18 was ectopically overexpressed in transgenic mice by using a liver-specific promoter to examine its functional effects in early development as well as in adult tissues. As shown in Table 2, ectopic hepatic overexpression of FGF-18 as a secretory protein in transgenic mice also induced proliferation in the liver, as evidenced by an increase in liver weight and total number of hepatocyte nuclei per unit area.

DISCUSSION

We have recently identified and isolated a novel mouse and human FGF family member, FGF-18, whose sequence is most similar to that of FGF-8 among the FGF family members. Although the amino acid sequence of mouse FGF-18 is nearly identical (99% identity) to that of human FGF-18, the nucleotide sequence is relatively less highly conserved (90% identity). Unlike FGF-1, FGF-2, and FGF-9 (31), which lack a secretory signal sequence, the first 26 amino acids of the human and mouse FGF-18 protein are hydrophobic residues that are predicted to be signal peptides for secretion. Moreover, FGF-18 contains two potential N-linked glycosylation sites, suggesting that it is a glycoprotein. Indeed, the FGF-18 protein was secreted as a glycoprotein into the tissue culture media when it was expressed in 293T cells (Fig. 4B). Several other FGF members have also been shown to be glycosylated, although the importance of glycosylation to their function is not well understood.

The purified rMuFGF-18 protein was biologically active in vitro. Like FGF-1 and FGF-2, rMuFGF-18 activated DNA synthesis and cell proliferation in the NIH 3T3 fibroblast cell line. However, its specific activity on NIH 3T3 cells was lower than that of FGF-2. This result suggests that fibroblasts may not be the primary physiological target cell type for FGF-18 or, alternatively, that FGF-18 may be less potent than FGF-2 in general.

It has been shown that FGFs often associate with the extracellular matrix/basement membrane polysaccharide HS (3, 25, 29, 37, 45, 46), and that HS is essential for the growth-stimulating activity of FGF-2 (17, 22, 34, 48). Therefore, we also examined whether HS was required for the proliferative effect of rMuFGF-18 on NIH 3T3 cells. Similar to the effect of HS on FGF-2, the proliferation-promoting activity of rMuFGF-18 was dependent on the presence of cell-associated HS. However, the functional role of HS in the matrix interactions of FGF-18 remains unknown.

To determine whether rMuFGF-18 was biologically active in vivo and to determine its functional role in animals, we used two independent approaches to examine its activity in mice. First, rMuFGF-18 protein was systemically administered to normal mice to examine its biological activity in vivo. Morphologic changes indicated that rMuFGF-18 induced proliferation in a wide variety of tissues of both epithelial and mesenchymal origin, effects which were somewhat similar to those induced by systemic administration of FGF-1 (8a). The epithelial proliferative effects were also somewhat similar to but considerably smaller than the effects induced by keratinocyte growth factor (KGF or FGF-7) (20). Nevertheless, the two tissues which appeared to be the primary targets of rMuFGF-18 were the liver and small intestine, both of which exhibited histologic evidence of proliferation and showed significant gains in weight after 7 (sometimes 3) days of rMuFGF-18 treatment. By using BrdU to access proliferative activity, the primary in vivo target cells for rMuFGF-18 were identified as hepatocytes. Additional sites of nuclear BrdU labeling were urinary bladder transitional urothelium, pancreatic ductal and acinar epithelium, smooth muscle cells in the tunica muscularis of the intestine and urinary bladder, and fibroblasts and smooth muscle cells in the pancreatic interstitium. The functional effects of increased labeling at these sites are unknown since morphologic evidence of cell proliferation (e.g., hyperplasia) was not evident in these tissues.

The second in vivo approach was to overexpress MuFGF-18 ectopically in transgenic mice by using a liver-specific promoter to examine its functional effects during development as well as in adult tissues. As expected, hepatic overexpression of MuFGF-18 protein induced a significant increase in liver weight as well as an increase in the total number of hepatocytes per unit area (Table 2). FGF-18-overexpressing transgenic mice did not exhibit any significant changes in the small intestine, suggesting that MuFGF-18 may not have reached the small intestine in sufficient quantities to induce proliferative changes. Thus, these two independent in vivo approaches yielded qualitatively similar but not identical effects.

The mechanism by which FGFs stimulate cell proliferation is thought to be mediated by a dual-receptor system, i.e., FGFR and HS proteoglycans (reviewed in references 11 and 25). The FGFR family consists of four distinct tyrosine kinase receptors and many isoforms of these receptors which are generated by alternative RNA splicing. Therefore, a number of the FGFR isoforms can bind several FGFs. At present, it is not clear whether FGF-18 binds to any known member of the FGFR family or whether it requires a novel receptor to transduce its proliferative signal into cells. Identification of the specific receptor for FGF-18 and its expression pattern in embryonic and adult tissues should help elucidate its physiological role. Furthermore, understanding the involvement of HS in the ligand-receptor interaction might clarify the observed effect of HS in the in vitro mitogenic assay.

In summary, we have identified, characterized, and studied the function of a novel member of the FGF family, FGF-18. FGFs are potent mitogens for a wide variety of cells of mesenchymal and neuroectodermal origin. Moreover, FGFs play a role in the differentiation of a variety of cells and are involved in morphogenesis, angiogenesis, and development. Thus, identification and characterization of a novel FGF may contribute to a better understanding of the role that FGFs play in normal development and pathologic processes.

ACKNOWLEDGMENTS

We thank B. Sutton for DNA sequencing; J. Speakman for the MTS cell proliferation assay; M. Chirica for large-scale production of *E. coli* protein; S. Hara and H. Lu for partial amino acid sequence determination; D. Chang for the BIAcore assay; E. Han for ELISA data analysis; J. Tarpley for configuring the image analysis program for

nuclear counts; D. Paulin and V. Gottmer for technical illustration; and R. Bosselman, T. Ulich, and L. Souza for their support.

REFERENCES

1. **Adnane, J., P. Gaudray, C. A. Dionne, G. Crumley, M. Jaye, J. Schlessinger, P. Jeanteur, D. Birnbaum, and C. Theillet.** 1991. BEK and FLG, two receptors to members of the FGF family, are amplified in subsets of human breast cancers. Oncogene **6:**659–663.
2. **Anandappa, S. Y., J. H. R. Winstanley, S. Leinster, B. Green, P. S. Rudland, and R. Barraclough.** 1994. Comparative expression of fibroblast growth factor mRNAs in benign and malignant breast disease. Br. J. Cancer **69:**772–776.
3. **Baird, A., and N. Ling.** 1987. Fibroblast growth factors are present in the extracellular matrix produced by endothelial cells *in vitro*: implications for a role of heparinase-like enzymes in the neovascular response. Biochem. Biophys. Res. Commun. **142:**428–435.
4. **Brinster, R. L., H. Y. Chen, M. E. Trumbauer, M. K. Yagle, and R. D. Palmiter.** 1985. Factors affecting the efficiency of introducing foreign DNA into mice by microinjecting eggs. Proc. Natl. Acad. Sci. USA **82:**4438–4442.
5. **Clarke, M. S. F., R. Khakee, and P. L. McNeil.** 1993. Loss of cytoplasmic basic fibroblast growth factor from physiologically wounded myofibers and dystrophic muscle. J. Cell Sci. **106:**121–133.
6. **Coulier, F., P. Pontarotti, R. Roubin, H. Hartung, M. Goldfarb, and D. Birnbaum.** 1997. Of worms and men: an evolutionary perspective on the fibroblast growth factor (FGF) and FGF receptor families. J. Mol. Evol. **44:**43–56.
7. **Crabb, J. W., L. G. Armes, S. A. Carr, C. M. Johnson, G. D. Roberts, R. S. Bordoli, and W. L. McKeechan.** 1986. Complete primary structure of prostatropin, a prostate epithelial cell growth factor. Biochemistry **25:**4988–4993.
8. **Cuevas, P., J. Burgos, and A. Baird.** 1988. Basic fibroblast growth-factor (FGF) promotes cartilage repair *in vivo*. Biochem. Biophys. Res. Commun. **156:**611–618.

8a. **Danilenko, D. M., and R. M. Housley.** Unpublished data.

9. **Esch, F., A. Baird, N. Ling, N. Ueno, F. Hill, L. Denoroy, R. Klepper, D. Gospodarowicz, P. Bolen, and R. Guillemin.** 1985. Primary structure of bovine pituitary basic fibroblast growth factor (FGF) and comparison with the amino-terminal sequence of bovine brain acidic FGF. Proc. Natl. Acad. Sci. USA **82:**6507–6511.
10. **Fernig, D. G., R. Barraclough, Y. Ke, M. C. Wilkinson, P. S. Rudland, and J. A. Smith.** 1993. Ectopic production of heparin-binding growth factors and receptors for basic fibroblast growth factor by rat mammary epithelial cell lines derived from malignant metastatic tumours. Int. J. Cancer **54:**629–635.
11. **Fernig, D. G., and J. T. Gallagher.** 1994. Fibroblast growth factors and their receptors: an information network controlling tissue growth, morphogenesis and repair. Prog. Growth Factor Res. **5:**353–377.
12. **Gospodarowicz, D.** 1974. Localisation of fibroblast growth factor and its effect alone and with hydrocortisone on 3T3 cell growth. Nature **249:**123–127.
13. **Gospodarowicz, D.** 1991. Fibroblast growth factors: from genes to clinical applications. Cell Biol. Rev. **25:**307–314.
14. **Gospodarowicz, D., G. Greenburg, and H. Bialecki.** 1978. Factors involved in the modulation of cell proliferation *in vivo* and *in vitro*: the role of fibroblast and epidermal growth factors in the proliferative response of mammalian cells. In Vitro **14:**85.
15. **Gospodarowicz, D., G. Neufeld, and L. Schweigerer.** 1986. Molecular and biological characterization of fibroblast growth-factor, an angiogenic factor which also controls the proliferation and differentiation of mesoderm and neuroectoderm derived cells. Cell Differ. **19:**1–17.
16. **Gospodarowicz, D., J. Plouet, and B. Malerstein.** 1990. Comparison of the ability of basic and acidic fibroblast growth factor to stimulate the proliferation of an established keratinocyte cell line: modulation of their biological effects by heparin, transforming growth factor β (TGFβ), and epidermal growth factor (EGF). J. Cell. Physiol. **142:**325–333.
17. **Guimond, S., M. Maccarana, B. B. Olwin, U. Lindahl, and A. C. Rapraeger.** 1993. Activating and inhibitory heparan sequences for FGF-2 (basic FGF). J. Biol. Chem. **268:**23906–23914.
18. **Halaban, R.** 1991. Growth factors and tyrosine protein kinases in normal and malignant melanocytes. Cancer Metast. Rev. **10:**129–140.
19. **Hattori, Y., H. Odagiri, H. Nakatani, K. Miyagawa, K. Naito, H. Sakamoto, O. Katoh, T. Yoshida, T. Sugimura, and M. Terada.** 1990. K-sam, an amplified gene in stomach cancer is a member of the heparin-binding growth factor receptor genes. Proc. Natl. Acad. Sci. USA **87:**5983–5987.
20. **Housley, R. M., C. F. Morris, W. Boyle, B. Ring, R. Biltz, J. E. Tarpley, S. L. Aukerman, P. L. Devine, R. H. Whitehead, and G. F. Pierce.** 1994. Keratinocyte growth factor induces proliferation of hepatocytes and epithelial cells throughout the rat gastrointestinal tract. J. Clin. Invest. **94:**1764–1777.
21. **Humphries, D. E., and R. L. Stevens.** 1992. Regulation of the gene that encodes the peptide core of heparin proteoglycan and other proteoglycans that are stored in the secretory granules of hematopoietic cells, p. 59–67. *In* D. A. Lane, I. Bjork, and U. Lindahl (ed.), Heparin and related polysaccharides. Plenum Press, New York, N.Y.
22. **Ishihara, M., D. J. Tyrrell, G. B. Stauber, S. Brown, L. S. Cousens, and R. J. Stack.** 1993. Preparation of affinity-fractionated, heparin-derived oligosaccharides and their effects on selected biological activities mediated by basic fibroblast growth factor. J. Biol. Chem. **268:**4675–4683.
23. **Jaye, M., R. Howk, W. Burgess, G. A. Ricca, I.-M. Chiu, M. Ravera, S. J. O'Brien, W. S. Modi, T. Maciag, and W. N. Drohon.** 1986. Human endothelial cell growth factor: cloning, nucleotide sequence and chromosome localization. Science **233:**541–545.
24. **Kimelman, D., J. A. Abraham, T. Haaparanta, T. M. Palisi, and M. W. Kirschner.** 1988. The presence of fibroblast growth-factor in the frog egg—its role is a natural mesoderm inducer. Science **242:**1053–1056.
25. **Klagsbrun, M., and A. Baird.** 1991. A dual receptor system is required for basic fibroblast growth factor activity. Cell **67:**229–231.
26. **Kornmann, M., T. Ishiwata, H. G. Beger, and M. Korc.** 1997. Fibroblast growth factor-5 stimulates mitogenic signaling and is overexpressed in human pancreatic cancer: evidence for autocrine and paracrine actions. Oncogene **15:**1417–1424.
27. **Li, D. C., J. Bell, A. Brown, and C. L. Berry.** 1994. The observation of angiogenin and basic fibroblast growth factor gene expression in human colonic adenocarcinomas, gastric adenocarcinomas, and hepatocellular carcinomas. J. Pathol. **172:**171–175.
28. **Luqmani, Y. A., M. Graham, and R. C. Coombes.** 1992. Expression of basic fibroblast growth factor, FGFR1 and FGFR2 in normal and malignant human breast, and comparison with other normal tissues. Br. J. Cancer **66:**273–280.
29. **Maccarana, M., B. Casu, and U. Lindahl.** 1993. Minimal sequence in heparin/heparan sulphate required for binding of basic fibroblast growth factor. J. Biol. Chem. **268:**23898–23905.
30. **Mason, I. J.** 1994. The ins and outs of fibroblast growth factors. Cell **78:**547–552.
31. **Miyamoto, M., K.-I. Naruo, C. Seko, S. Matsumoto, T. Kondo, and T. Kurokawa.** 1993. Molecular cloning of a novel cytokine cDNA encoding the ninth member of the fibroblast growth factor family, which has a unique secretion property. Mol. Cell. Biol. **13:**4251–4259.
32. **Peyrat, J. P., J. Bonneterre, H. Hondermarck, B. Hecquet, A. Adenis, M. M. Louchez, J. Lefebvre, B. Boilly, and A. Demaille.** 1992. Basic fibroblast growth-factor (bFGF)—mitogenic activity and binding-sites in human breast cancer. J. Steroid Biochem. Mol. Biol. **43:**87–94.
33. **Peyrat, J. P., H. Hondermarck, B. Hecquet, A. Adenis, and J. Bonneterre.** 1992. bFGF binding sites in human breast cancer. Bull Cancer **79:**251–260.
34. **Rapraeger, A. C., A. Krufka, and B. B. Olwin.** 1991. Requirement of heparan sulfate for bFGF-mediated fibroblast growth and myoblast differentiation. Science **252:**1705–1708.
35. **Ron, D., D. P. Bottaro, P. W. Finch, D. Morris, J. S. Rubin, and S. A. Aaronson.** 1993. Expression of biologically active recombinant keratinocyte growth factor. J. Biol. Chem. **268:**2984–2988.
36. **Rudland, P. S., W. E. Seifert, and D. Gospodarowicz.** 1974. Growth control and mitogenic response in cultured fibroblasts: induction of the pleiotypic and mitogenic response by a purified growth factor. Proc. Natl. Acad. Sci. USA **71:**2600–2604.
37. **Schlessinger, J., I. Lax, and M. Lemmon.** 1995. Regulation of growth factor activation by proteoglycans: what is the role of the low affinity receptors? Cell **83:**357–360.
38. **Shipley, G. D., W. W. Keeble, J. E. Hendrickson, R. J., Coffey, Jr., and M. R. Pittelkow.** 1989. Growth of normal human keratinocytes and fibroblasts in serum-free medium is stimulated by acidic and basic fibroblast growth factor. J. Cell. Physiol. **138:**511–518.
39. **Simonet, W. S., N. Bucay, S. J. Lauer, and J. M. Taylor.** 1993. A far-downstream hepatocyte-specific control region directs expression of the linked human apolipoprotein E and C-I genes in transgenic mice. J. Biol. Chem. **268:**8221–8229.
40. **Slack, J. M. W., H. V. Isaacs, and B. G. Darlington.** 1988. Inductive effects of FGF and lithium ion on *Xenopus* blastula ectoderm. Development **103:**581–590.
41. **Smith, J. A., D. Winslow, M. J. O'Hare, and P. S. Rudland.** 1984. Brain and pituitary fibroblast growth factor activities behave identically on three independent high performance liquid chromatography systems. Biochem. Biophys. Res. Commun. **119:**311–318.
42. **Tanaka, A., K. Miyamoto, N. Minamino, M. Takeda, B. Sato, H. Matsuo, and K. Matsumoto.** 1992. Cloning and characterization of an androgen-induced growth factor essential for the androgen-dependent growth of mouse mammary carcinoma cells. Proc. Natl. Acad. Sci. USA **89:**8928–8932.
43. **Theillet, C., X. Le Roy, O. De Lapeyriere, J. Grosgeorges, J. Adnane, S. D. Raynaud, J. Simony-Lafontaine, M. Goldfarb, C. Escot, D. Birnbaum, and P. Gaudray.** 1989. Amplification of FGF-related genes in human tumors: possible involvement of HST in breast carcinomas. Oncogene **4:**915–922.
44. **Thompson, J. D., D. G. Higgins, and T. J. Gibson.** 1994. CLUSTAL W: improving the sensitivity of progressive multiple sequence alignment through sequence weighting, position-specific gap penalties and weight matrix choice. Nucleic Acids Res. **22:**4673–4680.
45. **Turnbull, J. E., D. G. Fernig, Y. Ke, M. C. Wilkinson, and J. T. Gallagher.** 1992. Identification of the basic fibroblast growth factor binding sequence in fibroblast heparan sulphate. J. Biol. Chem. **267:**10337–10341.

46. **Vlodavsky, I., J. Folkman, R. Sullivan, R. Fridman, R. Ishai-Michaeli, J. Sasse, and M. Klagsbrun.** Endothelial cell-derived basic fibroblast growth factor: synthesis and deposition into subendothelial extracellular matrix. Proc. Natl. Acad. Sci. USA **84:**2292–2296.
47. **von Heijne, G.** 1986. A new method for predicting signal sequence cleavage sites. Nucleic Acids Res. **14:**4683–4690.
48. **Walker, A., J. E. Turnbull, and J. T. Gallagher.** 1994. Specific heparan sulphate saccharides mediate the activity of basic fibroblast growth factor. J. Biol. Chem. **269:**931–935.
49. **Wilcox, J. N.** 1993. Fundamental principles of in situ hybridization. J. Histochem. Cytochem. **41:**1721–1723.
50. **Wilkinson, M. C., M. J. Gardner, P. W. Gould, B. A. Taylor, and D. G. Fernig.** 1993. Normal and malignant human colonic mucosa contain acidic and basic fibroblast growth factors. Int. J. Oncol. **3:**933–936.